



Analyst

Monitoring gestational diabetes at the point-of-care via dual glycosylated albumin lateral flow assays in conjunction with a handheld reader

Journal:	<i>Analyst</i>
Manuscript ID	AN-ART-07-2022-001238.R1
Article Type:	Paper
Date Submitted by the Author:	21-Oct-2022
Complete List of Authors:	Belsare, Sayali; Texas A&M University, Biomedical Engineering Tseng, Derek; UCLA, EE Ozcan, Aydogan; University of California Los Angeles Cote, Gerard; Texas A&M University, Biomedical Engineering

SCHOLARONE™
Manuscripts

ARTICLE

Monitoring gestational diabetes at the point-of-care via dual glycosylated albumin lateral flow assays in conjunction with a handheld reader

Sayali Belsare,^{*a} Derek Tseng,^b Aydogan Ozcan,^{b,c} and Gerard Coté^{a,d}

Chronic conditions like diabetes require monitoring of vital biomarkers over extended periods of time. Monitoring gestational diabetes mellitus (GDM) is crucial to avoid short- and long-term adverse effects on both mother and infant. Providing monitoring systems to patients at the point-of-care (POC) has the potential to help mitigate these effects. In this manuscript, we propose the use of a sensing system combining lateral flow assays (LFAs) with a handheld colorimetric reader for use in tracking the glycemic status of a GDM patient at the POC. Current strategies of GDM monitoring include glucose and HbA1c measurements. These are often too frequent or not frequent enough for effective monitoring. Hence, we have developed a sensor for an intermediate interval biomarker – glycosylated albumin (GA). Based on the half-life of the protein, GA is measured once every 2-3 weeks. Here we first present two lateral flow assays, one for GA and another for total serum albumin used in conjunction with a handheld reader to read the colorimetric signals. Both assays have a sandwich aptamer format and measure the target proteins in their physiologically relevant ranges. The GA assay has a dynamic range of 3-20mg/ml and the serum albumin assay has a range of 20-50mg/ml without any sample dilution. Both LFAs were then incorporated into a single dual assay cartridge such that both assays could run simultaneously and provide the % glycosylated albumin value from a single test. Thus, the dual assay cartridge plus reader system has the potential to provide an effective platform for measuring GA for tracking GDM at the POC.

Introduction

Gestational Diabetes Monitoring

Gestational diabetes is the third most prevalent type of diabetes mellitus after Type I and Type II diabetes¹. As the name suggests, it affects women during pregnancy. GDM most commonly develops between the 24th to 28th week of pregnancy^{1,2} and has a range of short and long-term adverse effects on both the pregnant woman and foetus. The short-term effects to the patient include pre-eclampsia, shoulder dystocia and increased risk of C-section³. Short-term effects on the infant include neonatal hypoglycemia and neonatal jaundice. Further, type II diabetes may develop in both mother and infant in the long term⁴. To avoid these effects, it is crucial to monitor GDM carefully during pregnancy up to a couple of months after the baby is born.

Currently, the standard strategy to monitor GDM is direct glucose measurement and/or HbA1c measurement. Due to the rate of glucose metabolism, it is typically recommended that patients with diabetes measure it 4-5 times a day. Since GDM is primarily characterized by consistent hyperglycemia⁵ with rare hypoglycemic

episodes, multiple glucose measurements may not always be necessary. Since the recommendation is multiple readings per day, traditional glucose meters would require multiple fingerpicks every day, which can result in non-compliance from the patients' side. The other standardized biomarker for diabetes is glycosylated hemoglobin (HbA1c)⁶. Due to its longer half-life, HbA1c is measured only once in 2-3 months⁷. In this case, the longer timeline is not ideal since the crucial monitoring period for GDM is about 6-7 months. Hence, specifically for GDM, an intermediate biomarker (interval: 2 weeks) would be advantageous for monitoring glycemic status. It would also be useful for monitoring the effects of therapeutic strategies like alterations in dietary regimens and exercise routines⁸.

One such intermediate interval biomarker is glycosylated albumin (GA)^{9,10}. Free glucose in the bloodstream binds to serum albumin via non-enzymatic glycation reaction to form glycosylated albumin¹¹. It reflects glycemic excursions of postprandial plasma glucose along with average plasma glucose¹². Since glycosylated albumin is reported as a ratio of glycosylated to total albumin, unglycosylated protein also has to be measured in addition to the glycosylated version. In normal conditions, about 10 to 16% of serum albumin is glycosylated¹⁰. However, in cases of prolonged hyperglycemia, up to 40% of albumin can be glycosylated¹⁰. Since glycation of albumin as a phenomenon is not restricted to GDM, as a biomarker, it can be used to monitor type I and type II diabetes as well¹³.

^a Department of Biomedical Engineering, Texas A&M University, College Station, TX

^b Electrical and Computer Engineering Department, University of California, Los Angeles, CA

^c Bioengineering Department, University of California, Los Angeles, CA

^d Texas Engineering Experiment Station Centre for Remote Health Technologies and Systems, College Station, TX

*Corresponding author email: sayali22@tamu.edu

Point-of-Care Monitoring with Lateral Flow Assays

In the past two years, COVID-19 has demonstrated the importance of point-of-care (POC) tests. Testing at home is not just convenient for patients but also plays a major role in relieving the load on healthcare providers^{14–16}. Most commercially available at-home tests like Panbio rapid test (Abbott) or SD Biosensor rapid test (Roche) use the standard lateral flow assay (LFA) design¹⁷. Lateral flow assays are one of the most established forms of paper based POC test platforms^{18,19}. Their compact size, portability, low-cost and ease-of-use make them ideal candidates for POC applications. To date, several LFAs have been developed for a range of applications like COVID-19, influenza, bacterial pathogens, heart failure etc.^{18,20–22}.

The principal components of any LFA typically include recognition elements like antibodies^{23,24} for the capture of the target biomolecule onto the test strip and transduction elements like enzymes^{25,26} or nanoparticles^{21,23} to transduce the recognition event into a readable signal. Antibodies have been established as recognition elements in lateral flow assays owing to their high sensitivity and specificity^{27,28}. However, they also have drawbacks like high cost of production and thermal instability. On the other hand, aptamers, which are single-stranded DNA or RNA sequences, also have the potential to be used as recognition elements for LFAs due to their thermal stability, stability over a range of pH, low-cost and longer shelf life^{29,30,31} which make them more suited for use in point-of-care tests.

The other main component of any biosensor is the transduction element. For qualitative POC tests, the signal generated by the transduction element can be observed visually to get a yes/no answer³². However, for quantitative tests, the transduced signal must be measured and quantified^{24,33}. Several optical techniques like colorimetry³⁴, fluorescence³⁵ and surface-enhanced Raman spectroscopy³⁶ have been explored for lateral flow applications. The use of bare gold nanoparticles for colorimetric signal generation is a sensitive and cost-effective optical transduction technique since it does not require any dye and uses less sophisticated equipment for signal generation and measurement^{37–40}.

Ikeda et al.⁴¹, Testa et al.⁴², and Ko et al.⁴³ have published assays for glycosylated albumin detection using various enzymatic methodologies. Inoue et al.⁴⁴, and Bohli et al.⁴⁵ have published enzyme and antibody-based sensors using electrochemical detection methods. Ki et al.^{46,47} have published colorimetric antibody-based assays to measure glycosylated and serum albumin. Apiwat et al.⁴⁸ and Gosh et al.⁴⁹ have published fluorescence-based detection systems with aptamers as the recognition elements. While successfully detecting and measuring glycosylated albumin, all these systems have certain limitations in terms of POC applications. Enzymes and antibodies have low thermal stability and hence require low-temperature storage for effective use. Transduction methods like electrochemistry are not ideal for POC application since the associated equipment is likely not compact or portable. Lastly, most

of the above-mentioned assays require an additional dilution step for sensing due to high concentrations of the target proteins. The current and only commercial standard for GA is the Lucica GA-L assay⁵⁰. While this assay is a commercial standard, it is a lab-based enzymatic assay which uses clinical analysers.

In this manuscript, a sensing system has been developed for monitoring gestational diabetes at the point-of-care using glycosylated albumin as the target biomarker. The sensing system is comprised of a dual assay cartridge consisting of two aptamer-based sandwich assays on lateral flow platforms, for glycosylated and serum albumin (Fig. 1(a)). Initially both assays were developed separately, and their results have been reported. That was followed by incorporation of both assays into a single dual assay cartridge to run both assays simultaneously. The signal generated by the assays was read using a custom handheld colorimetric reader (Fig. 1(b), (c), (d)) following our earlier designs^{51,52}. The combination of lateral flow tests with a compact reader satisfies the RE-ASSURED criteria set by World Health Organization (WHO) for point-of-care testing⁵³. The combination of dual lateral flow assay cartridge and the handheld reader was designed specifically for simultaneous measurement of both forms of albumin (glycosylated and total) such that the % glycosylated albumin value can be obtained by the patient in 30 mins at-home without diluting the samples.

Materials and Methods

Materials

Gold (III) chloride trihydrate (HAuCl_4) and tri-sodium citrate dihydrate ($\text{Na}_3\text{C}_5\text{H}_7\text{O}_7$) for gold nanoparticle synthesis were purchased from MilliporeSigma (St. Louis, MO). Syringe filters (0.2 μm) were purchased from VWR (Pennsylvania, USA). All five aptamers were purchased from Integrated DNA Technologies (Iowa, USA). The oligonucleotide sequences are listed in the supplemental information (Table S1). Tris (2-carboxyethyl) phosphine hydrochloride (TCEP), sodium chloride (NaCl) and phosphate-buffered saline (PBS; pH 7.4) tablets were purchased from Sigma. Nanosep centrifugal filters were purchased from Pall Corporation (New York, USA). Serum albumin, glycosylated albumin and glucose were purchased from Sigma. Simulated blood serum (without albumin) was purchased from Biochemazone (Edmonton, Canada). Milli-Q deionized (DI) water (18.2 $\text{M}\Omega\text{cm}^{-1}$) was used in all experiments. Whatmann G4 chromatography paper and nitrocellulose membrane (FF170HP) were purchased from Cytiva (Marlborough, MA). Glass fiber membrane was purchased from EMD Millipore (Burlington, MA). Thick absorbent paper (Trans-blot filter paper) was purchased from BioRad (Hercules, CA). Lateral flow cartridges and backing cards were purchased from DCN Dx (San Diego, CA). ESun pla+ filament was purchased from Amazon. UV-Visible spectrometry was conducted using a Tecan Infinite 200 Pro (Männedorf, Switzerland) plate reader.

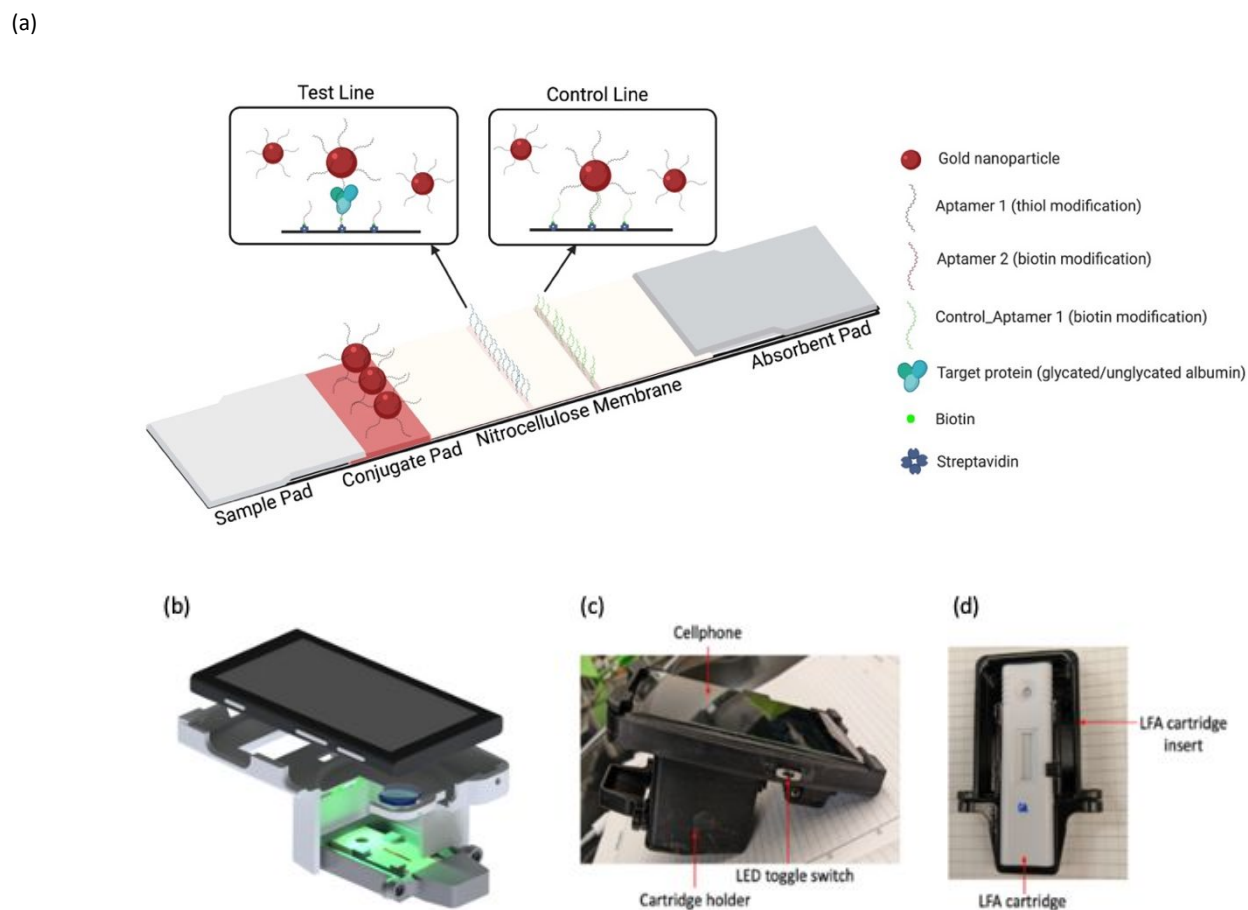


Fig. (1) (a) Lateral flow assay schematic (Created with BioRender.com) (b) Handheld colorimetric reader (CAD design); (c) Handheld colorimetric reader and (d) lateral flow assay cartridge holder

Zeta potential and dynamic light scattering measurements were conducted on a Zetasizer Nano ZS90 (Malvern, UK). Dual assay cartridges were printed on a Prusa i3 mk3s+ printer. Colorimetric measurements were performed using a custom handheld reader developed by our team.

Methods

Synthesis and characterization of gold nanoparticles. Gold nanoparticles were synthesized using the protocol published by Bastus et al.⁵⁴ Briefly, 1ml of 110mM sodium citrate was added to 49ml of boiling DI water. Two minutes after citrate addition, 335 μ l of 25mM gold chloride was added. The solution was allowed to boil for 15-20mins for seed formation. Once the solution turned ruby red, the temperature was reduced and maintained at 90 $^{\circ}$ C for the remainder of the synthesis. After 1 hour, particle size was measured via absorbance measurements. If the size was insufficient, 335 μ l of 60mM sodium citrate was added, followed by 335 μ l of gold chloride. This step was repeated until the desired nanoparticle size was

obtained. After the synthesis process, the nanoparticles were filtered using a 0.2 μ m syringe filter to remove aggregates. Filtered particles were stored at 4 $^{\circ}$ C until further use. The size and diameter of the particles were calculated from the absorbance spectrum. Hydrodynamic size was confirmed using dynamic light scattering. Zeta potential of the particles was also measured.

Conjugation of aptamers. Aptamers selective to glycated albumin and human serum albumin were conjugated to gold nanoparticles via thiol modifications on the aptamers (aptamer sequences listed in Table S1). Selectivity of the aptamers was previously tested and confirmed by our group⁵⁵. The aptamers purchased from Integrated DNA Technologies had a disulphide bond which was reduced before conjugation. This was achieved by adding 20mM TCEP to the aptamers. After a one-hour incubation, the excess was removed by washing with a Nanosep centrifugal filter (10kDa MWCO). The aptamers were finally resuspended to the original volume and folded by heating in a water bath at 85 $^{\circ}$ C. The concentrations of the

1
2
3 aptamers were measured via absorbance measurements. Both
4 aptamers were added to separate batches of gold nanoparticles in
5 their respective ratios (3000:1 for the glycosylated albumin assay and
6 2000:1 for the serum albumin assay). The aptamer-nanoparticle
7 binding was carried out for one hour in a shaker and then left on the
8 benchtop overnight. Salt aging was conducted after incubation using
9 2M NaCl⁵⁶. After salt addition was complete, particles were left on
10 the benchtop overnight. The particles were then centrifuged at 10k
11 rcf to remove the unbound aptamers and resuspended in 1X PBS.
12 Particles were resuspended to a final OD 1 for the glycosylated albumin
13 assay and OD 1.5 for the serum albumin assay. These particles were
14 then stored at room temperature on the benchtop until further use.

15
16
17 **Lateral flow assay (LFA) design.** Lateral flow assay components used
18 in this work followed the standard LFA design^{27,30,57,58}. Capture
19 aptamer and control aptamers (sequences in Table S1) were
20 purchased with biotin modifications. The biotinylated aptamers were
21 conjugated to streptavidin and immobilized onto the nitrocellulose
22 membrane using a lateral flow dispenser. The striped aptamer was
23 dried in a desiccator overnight. Glass fibre membrane was used for
24 conjugate storage. It was pre-treated with 1X PBS + 0.7% casein + 7%
25 sucrose + 0.05% Tween-20. Aptamer conjugated nanoparticles were
26 loaded onto the glass fibre membrane and dried in a desiccator
27 overnight. G4 chromatography paper, used as the sample pad, was
28 pre-treated with 1X PBS + 5% sucrose + 0.25% Tween-20. A thick
29 trans blot absorbent pad was used to absorb excess sample, buffer,
30 and nanoparticles. The chromatography paper, glass fibre
31 membrane, nitrocellulose membrane and absorbent pad were
32 attached to the backing card with a 2mm overlap between
33 consecutive layers (Fig. 1(a)). The backing card with the assembled
34 lateral flow layers was placed into the cartridge, after which the test
35 was ready to run. Cutting, pre-treatment of membranes and
36 assembly of the lateral flow strip were all a part of construction of
37 the strips. All buffer formulations and membranes were identical for
38 both glycosylated and serum albumin assays.

39
40
41 **Handheld reader design.** The reader was built based on the design
42 of Mudanyali et al.⁵¹ A Nokia Lumia 1020 was used for the reader to
43 capture images of the lateral flow test strips. A 20mm diameter
44 biconvex lens with a focal length of ~30mm, was placed in front of
45 the existing camera module of the smartphone, while the lateral flow
46 test strips were placed ~35mm away from the smartphone camera.
47 Lateral flow test strips were illuminated using two LEDs as the light
48 source (SunLED XSFWCB983W and Broadcom Limited ALMD-CM3F-
49 Y1002), which were powered by two AAA batteries with a slide
50 switch to turn it on / off. The mechanical body of the reader (Fig. 1(c))
51 was fabricated using the Stratasys Objet30 Pro 3D printer, which uses
52 VeroBlackPlus photo resin as the building material to hold the
53 smartphone, external lens, and its electrical components. A
54 customized test-holder tray (Fig. 1(d)) was also designed specifically
55 for the lateral flow test strip cartridge used in this work. This
56 customized test tray was mounted with magnets to help secure the
57 tray's position on the body of the reader.

Assay response and colorimetric measurement. Both lateral flow
assays were run by adding 30µl of the sample followed by the
addition of 50µl running buffer (1X PBS + 0.1% Tween-20) after
5mins. Thirty minutes after sample addition (optimization in next
section), the signal was read using the handheld reader. The LFA
cartridge was placed into its holder, which was then inserted into the
reader. Once the holder was in place, the green LED (optimization in
next section) was turned on and the image was captured. The images
were then analysed using Image J software to get colorimetric
intensities.

Determination of assay run time: The run time of the assay was the
time interval measured starting from the addition of the sample to
the development of a constant signal intensity at the test line. It
determined by measuring the colorimetric signal intensity at
different time points after sample addition: 5mins, 10mins, 20mins,
30mins, 40mins and 50mins.

Determination of colorimetric channel: The custom handheld reader
was designed with two inbuilt LEDs: white and green. The ideal
colorimetric channel was determined by capturing images with both
white and green LED and analysing and comparing all colorimetric
channels from both LEDs. The ideal channel was chosen to be the one
that gave the highest signal sensitivity from lowest to highest target
concentrations for both assays.

Assay response in serum. The response of both assays was tested in
doped serum samples to evaluate their performance in a complex
biological fluid. The simulated serum was doped with 8 and 20mg/ml
glycosylated albumin and 35 and 50mg/ml serum albumin. 30µl of
the spiked samples was then added to the test strip followed by 50µl of
running buffer (1x PBS + 0.1% tween-20). The handheld reader was
then used to measure the signal at each test line. Each sample was
tested in triplicate.

Dual assay cartridge design. The dual assay cartridge was designed
in Solidworks and 3D printed in the lab. Two lateral flow assay strips:
one for glycosylated albumin assay and the other one for serum albumin
assay were placed on each side of the dual assay cartridge. Individual
lateral flow assay strips were constructed with the same membranes
and formulations as mentioned above. A G4 chromatography
membrane pre-treated with 1x PBS+5% sucrose+0.25% Tween-20
was placed as the connector between both assays.

Dual assay response. The symmetry of flow in dual assay cartridge
was first tested by placing glycosylated albumin assay strips in both
channels of the dual cartridge. 50µl of (20mg/ml glycosylated albumin)
sample was added to the inlet followed by 50µl of running buffer.
The assay signals were read, and the intensities plotted and
compared for both assays in the cartridge. Next, 50µl of sample

(S1/S2/S3) was added to the sample inlet to run both assays simultaneously. Sample 1 consisted of 3.5mg/ml GA and 25mg/ml HSA; sample 2 was comprised of 10mg/ml GA and 30mg/ml HSA;

sample 3 was a mix of 20mg/ml GA and 30mg/ml HSA. All samples were made by doping simulated blood serum with respective combinations of glycated and serum albumin.

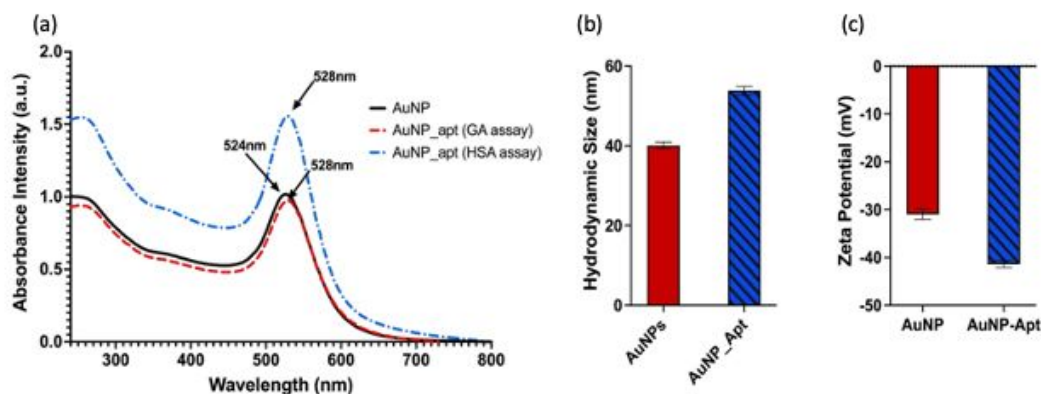


Fig. (2) (a) Absorbance spectrum of citrate capped AuNPs and aptamer conjugated AuNPs (GA assay and HSA assay); (b) Hydrodynamic sizes of nanoparticles before and after conjugation; (c) Zeta potential of particles before and after aptamer conjugation

Five mins after sample addition, 50 μ l of running buffer (1xPBS +0.1% Tween-20) was added to push all residual conjugates from the conjugate layers and flow through the nitrocellulose membrane. Colorimetric intensities were measured 30mins after sample addition. Each sample was tested in triplicate.

Results and Discussion

Nanoparticle characterization

Gold nanoparticles were synthesized by the seed growth method as described above. After synthesis was completed, the absorbance of the nanoparticles was measured using a plate reader. Using the absorbance spectrum, the size and concentration of the nanoparticles was calculated. The spectrum, as seen in Fig 2(a), has an absorbance peak at 524nm, which was used to calculate the size of the nanoparticles. These 40nm nanoparticles were used in all experiments. After both aptamers were conjugated to separate sets of nanoparticle solutions, conjugation was confirmed using via absorbance measurements. An absorbance peak shift of 4nm confirmed aptamer conjugation onto the nanoparticles for both assays. The peak shifts can be observed in Fig. 2(a). OD 1 particles were used for the glycated albumin assay, while OD 1.5 particles were used in the serum albumin assay owing to the higher concentration range. Nanoparticle size and conjugation was further confirmed by measuring the zeta potential and hydrodynamic size. As seen in Fig. 2(b), a 10nm increase in hydrodynamic size was observed after conjugation and a reduction of zeta potential from -31mV to -42mV was also seen (Fig. 2(c)).

Assay Response

Determination of assay run time. The time interval for measurement of assay response was determined by measuring the signal intensities over a period of 50 min. As seen in Fig. 3(a), the intensity reached 90% of the maximum intensity in 20mins. Maximum signal intensity was reached at the 30min time point, after which it stabilized. Hence, both assays were run for 30mins after which the final colorimetric intensities were measured. This was a marked improvement over the dipstick assays published by our group previously, in which signal development took between 60-75mins. The assay run time was measured for both glycated and serum albumin assays and 30mins was found to be the ideal run time for both assays.

Determination of colorimetric channel. The handheld reader used to measure colorimetric intensities was designed with two LEDs: white and green. Both assay responses were measured by capturing and analysing images using both LEDs to determine the optimum LED and channel to be used. As seen in Fig. 3(b), all three channels from the white LED as well as the green LED responded to the changing concentrations of the target protein. While the overall intensities of the colorimetric signals from the white LED images were higher, which was expected given the higher power of the white LED, it was observed that the green LED provided the highest sensitivity across the dynamic range, even higher than the green channel of the white LED. Hence, all intensity measurements for both assays were performed via green LED image captures. The colorimetric intensity measurements were performed for both assays and the green LED was observed to provide the best sensitivity for both assays.

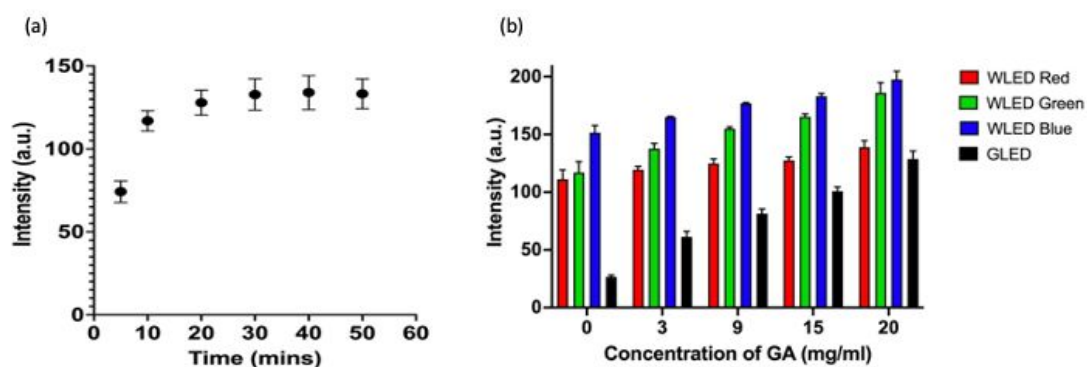


Fig. (3) (a) Development of colorimetric assay response signal intensity over time ($n=3$); (b) Colorimetric intensities of R-G-B channels (white LED) and green channel (green LED)

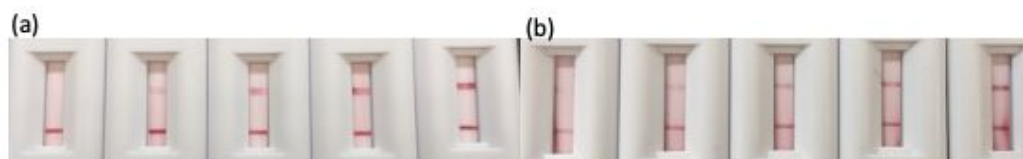


Fig. (4) Qualitative response for (a) glycated albumin and (b) serum albumin assays

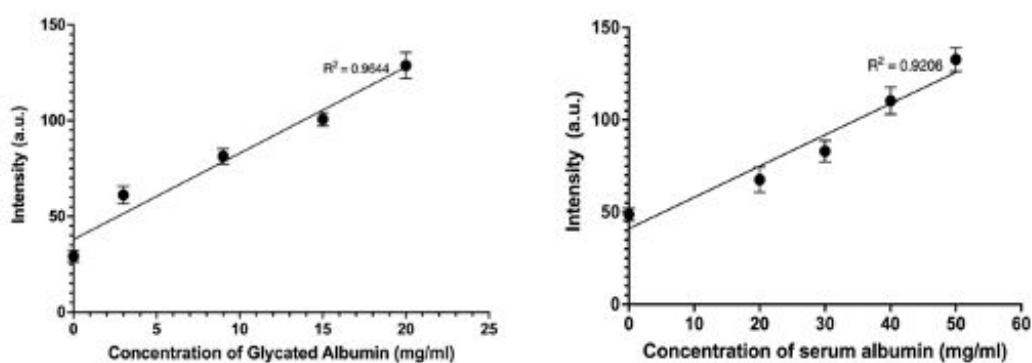


Fig. (5) Quantitative response (calibration curves) for (a) glycated albumin and (b) serum albumin assays

Once the assay parameters were finalized, both assays were run to obtain responses in the relevant concentration ranges. Since the assays are colorimetric, qualitative responses of both assays were obtained and can be visually observed in Fig. 4(a) and (b). Intensities of colorimetric signals at the test lines (first red line) increased as the concentration of the target protein increased. However, for monitoring purposes, a qualitative result provides insufficient information since knowledge of disease severity is required. It has been established that up to 16% glycated albumin indicates a healthy non-diabetic person¹⁰. However, if the % GA value is much higher, it indicates the need for intervention from healthcare professionals by prescribing alternative dietary or exercise regimens. Quantitative results were obtained by conducting analyses of images obtained using the handheld reader. The quantitative responses (calibration curves) in Fig 5(a) and (b) were obtained by analysing images from the green LED, 30 min after sample addition. Each concentration was tested in triplicate. A dynamic range of 3-20mg/ml was achieved for the glycated albumin assay and 20-50mg/ml for the serum albumin assay. It was observed from the plots that both assays have a linear correlation with the concentrations of the target proteins. Regression parameters for both assays have been listed in the supplementary information (Table S2). Based on these parameters, the LoD for the glycated albumin assay was calculated to be 0.8mg/ml and for the serum albumin assay was 1.5mg/ml.

Assay response in serum

Simulated blood serum was used to evaluate the response of both assays in a complex biological matrix. The serum was purchased without any albumin to control the amount of glycated and serum albumin present. This enabled the creation of samples containing different concentrations of glycated albumin and serum albumin to test both assays. The results are listed in Table (1) below. It can be observed that the recoveries are in the range of 93% to 104%, which implies that serum components do not have a major effect on the assays. Serum dilution was not required for either assay due to the

running buffer volume of 50 μ l, which was instrumental in improving the flow and overcoming the higher complexity of the serum by preventing non-specific binding.

Dual assay response

After both assays were optimized for the individual lateral flow configuration and tested in a complex biological medium, the final step was to incorporate them into a single cartridge. The dual assay cartridge was designed to enable the user to run both assays simultaneously and generate the % glycated albumin result in a single test instead of having to run two separate tests with two separate samples. The cartridge was designed in Solidworks and 3D printed in the lab. Fig. 6(a) illustrates the design of the cartridge. Fig. S1 includes top and bottom views of the cover and bottom of the cartridge. After designing and printing the cartridges, the symmetry of flow to both sides of the cartridge was confirmed by measuring and comparing signals for the same assay on both sides of the cartridge. It can be observed from Fig. 6(b) that signal intensities of assays on both sides of the cartridge were comparable implying that similar sample volumes flowed on both sides of the assays. Once flow symmetry was confirmed, dual assay response was tested via three samples with varying concentrations of glycated and serum albumin: S1 consisted of 3.5mg/ml GA and 25mg/ml HSA; S2 was comprised of 10mg/ml GA and 30mg/ml HSA; S3 was a mix of 20mg/ml GA and 30mg/ml HSA. The concentration levels were chosen such that the dynamic range of each assay was covered between the three samples. Fig. 7 demonstrates the dual assay response for all levels. Concentration levels of sample one (GA: 3.5mg/ml and SA: 25mg/ml) were chosen to demonstrate that lowest concentrations of both assay dynamic ranges could be successfully detected in the dual assay system. Sample 1 was equivalent to 12% glycation which corresponded to a non-diabetic healthy person. The second sample was at the mid-point of the glycated albumin assay range. For the serum albumin assay, the total serum albumin concentrations combined was equivalent to the mid-point of its dynamic range.

Table (1): Detection of target proteins in serum

Sample	Doped (mg/ml)	Recovered (mg/ml)	Recovery (%)	SD
GA 1	8	8.25	103.15	4.87
GA 2	20	19.48	97.4	2.7
HSA 1	35	33	94.28	3.61
HSA 2	50	46.89	93.78	4.04

This sample corresponded to 25% glycation which was comparable to mild to moderately severe diabetes. Finally, in the last sample, the concentration of glycated albumin was chosen to the upper limit of the dynamic range and serum albumin concentration was chosen such that the summation of both concentrations was equivalent to the highest relevant concentration for serum albumin. It was a 40% glycation sample which corresponded to a severely diabetic condition. In sample 3, unglycated serum albumin concentration was maintained at the same concentration as sample 2 to demonstrate that only an increase in glycated albumin could also be detected by the serum albumin assay. It was observed that there was a 7-10% increase in signal intensities compared to individual assays run separately. However, this was expected since in case of the glycated

albumin assay, non-specific binding from unglycated serum albumin to a small extent was anticipated. And in case of the serum albumin assay, aptamer binding to unglycated and glycated albumin was expected to differ to some extent resulting in minor differences in resultant signal intensities even at the same concentrations. In addition, all samples were doped in simulated blood serum which also contributed to the non-specific binding albeit to a small extent. However, it was noted that signal intensities for all concentration levels increased to a similar extent and hence the dual assay cartridge could in fact successfully be used to simultaneously measure glycated and total serum albumin to obtain the % glycated albumin value from a single sample and single test.

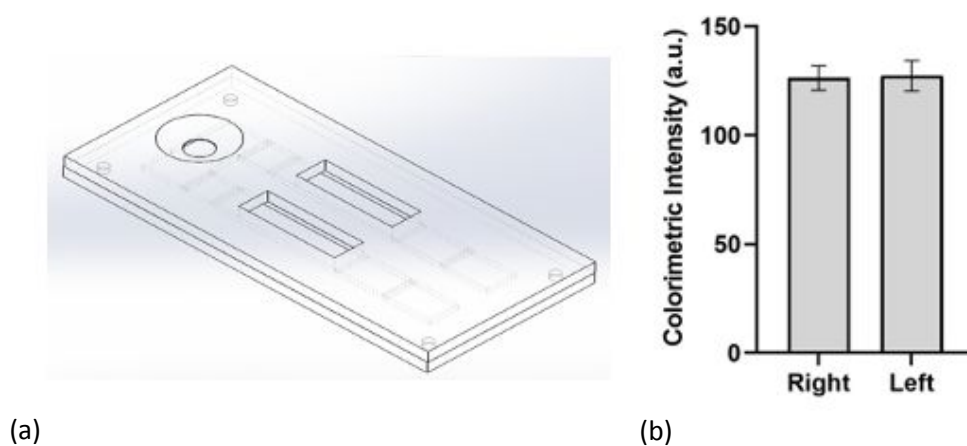


Fig. 6 (a) Dual assay cartridge design; (b) symmetry of flow in both channels of dual assay cartridge

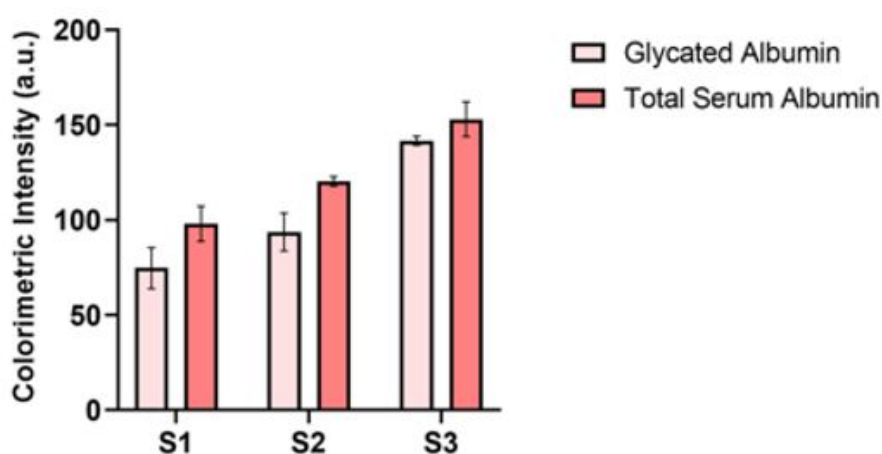


Fig. 7 Dual assay response (S1: 3.5mg/ml GA+25mg/ml HSA; S2: 10mg/ml GA+30mg/ml HSA; S3: 20mg/ml GA+30mg/ml HSA)

Conclusion

In this manuscript, two aptamer-based lateral flow assays were developed to measure glycated albumin and serum albumin in their relevant concentration ranges. The choice of aptamers was made over other recognition elements owing to their thermal stability, low cost, and relatively long shelf life. Both assays used gold nanoparticle-based colorimetry since it does not require any additional use of dyes which lowered the overall cost of the system. Both assays were immobilized onto lateral flow platforms, which afforded advantages like compact size, portability, and ease-of-use. A handheld colorimetric reader developed by the team was used in conjunction with lateral flow cartridges. When the sample was added to the cartridge, the target protein interacted and bound to the aptamer on the gold nanoparticles which were stored in the conjugate layer. The protein-particle complexes then flowed onto the nitrocellulose membrane, where they were captured at the test line. The number of particles at the test line was proportional to the concentration of the target protein in the sample, which was observed in the assay responses. The dynamic ranges for both assays were 3-20mg/ml and 20-50mg/ml, which are both physiologically relevant, implying that sample dilution will not be required to run the

assays. Finally, a dual assay cartridge was used to run both assays simultaneously to obtain the value of % glycated albumin from a single test. In conclusion, this research demonstrated that a dual lateral flow assay plus handheld colorimetric reader setup can effectively monitor glycated and serum albumin for ultimate use as a point-of-care sensor for monitoring gestational diabetes.

Conflicts of Interests

There are no conflicts to declare.

Acknowledgements

This research was supported by the National Science Foundation Precise Advanced Technologies and Health Systems for Underserved Populations (PATHS-UP) Engineering Research Center through award no. EEC-1648451. The authors would also like to acknowledge the discussions with Dr. Samuel Mabbott on lateral flow assay optimization.

References

1. American Diabetes Association. Gestational Diabetes Mellitus. *Diabetes Care*. 2004;27(SUPPL. 1). doi:10.2337/diacare.27.2007.S88
2. Kaaja R, Rönnemaa T. Gestational diabetes: Pathogenesis and consequences to mother and offspring. *Review of Diabetic Studies*. 2008;5(4):194-202. doi:10.1900/RDS.2008.5.194
3. Yogeve Y, Xenakis EMJ, Langer O. The association between preeclampsia and the severity of gestational diabetes: The impact of glycemic control. *Am J Obstet Gynecol*. 2004;191(5):1655-1660. doi:10.1016/j.ajog.2004.03.074
4. Maryland. Mild Traumatic Brain Injury (mTBI) / Concussion Policy and Management Plan. Published online 2015:2-21.
5. Kühl C, Hornnes PJ, Andersen O. Etiology and Pathophysiology of gestational diabetes mellitus. *Diabetes*. 1985;34(2):66-70. doi:10.1021/ma9704673
6. Renz PB, Cavagnoli G, Weinert LS, Silveiro SP, Camargo JL. HbA1c test as a tool in the diagnosis of gestational diabetes mellitus. *PLoS One*. 2015;10(8):1-11. doi:10.1371/journal.pone.0135989
7. Sherwani SI, Khan HA, Ekhzaimy A, Masood A, Sakharkar MK. Significance of HbA1c test in diagnosis and prognosis of diabetic patients. *Biomark Insights*. 2016;11:95-104. doi:10.4137/Bmi.s38440
8. Management of diabetes in pregnancy: Standards of medical care in Diabetes-2018. *Diabetes Care*. 2018;41(January):S137-S143. doi:10.2337/dc18-S013
9. Huang Y, Hu Y, Ma Y, Ye G. Glycated albumin is an optimal biomarker for gestational diabetes mellitus. *Exp Ther Med*. 2015;10(6):2145-2149. doi:10.3892/etm.2015.2808
10. Kohzuma T, Yamamoto T, Uematsu Y, Shihabi ZK, Freedman BI. Basic performance of an enzymatic method for glycated albumin and reference range determination. *J Diabetes Sci Technol*. 2011;5(6):1455-1462. doi:10.1177/193229681100500619
11. Sirangelo I, Iannuzzi C. Understanding the role of protein glycation in the amyloid aggregation process. *Int J Mol Sci*. 2021;22(12). doi:10.3390/ijms22126609
12. Koga M. Glycated albumin; clinical usefulness. *Clinica Chimica Acta*. 2014;433:96-104. doi:10.1016/j.cca.2014.03.001
13. Roohk HV, Zaidi AR. A Review of Glycated Albumin as an Intermediate Glycation Index for Controlling Diabetes. *J Diabetes Sci Technol*. 2008;2(6):1114-1121. doi:10.1177/193229680800200620

Analyst

ARTICLE

- 1
2
3
4
5 14. Price CP, St John A. Will COVID-19 be the coming of age for point-of-care testing? *BMJ Innov.* 2021;7(1):3-5. doi:10.1136/bmjinnov-2020-000466
6
7
8 15. O’Kane MJ. Patient self-testing in chronic disease management. *Journal of Laboratory Medicine.* 2020;44(2):81-87. doi:10.1515/labmed-2019-0175
9
10
11 16. Dunlap D, Ding E, Abramo K, et al. Point-of-care testing, your cardiologist, and affairs of the
12 heart. *Cardiovasc Digit Health J.* 2021;2(6):331-335. doi:10.1016/j.cvdhj.2021.10.004
13
14
15 17. Corman VM, Haage VC, Bleicker T, et al. Comparison of seven commercial SARS-CoV-2 rapid
16 point-of-care antigen tests: a single-centre laboratory evaluation study. *Lancet Microbe.*
17 2021;2(7):e311-e319. doi:10.1016/S2666-5247(21)00056-2
18
19
20 18. Zhou Y, Wu Y, Ding L, Huang X, Xiong Y. Point-of-care COVID-19 diagnostics powered by
21 lateral flow assay. *Trends in Analytical Chemistry.* 2021;145(116452).
22
23 19. Pohanka M. Point-of-Care Diagnoses and Assays Based on Lateral Flow Test. *Int J Anal*
24 *Chem.* 2021;2021. doi:10.1155/2021/6685619
25
26 20. Le TT, Chang P, Benton DJ, McCauley JW, Iqbal M, Cass AEG. Dual Recognition Element
27 Lateral Flow Assay Toward Multiplex Strain Specific Influenza Virus Detection. *Anal Chem.*
28 2017;89(12):6781-6786. doi:10.1021/acs.analchem.7b01149
29
30
31 21. Wang R, Kim K, Choi N, et al. Highly sensitive detection of high-risk bacterial pathogens
32 using SERS-based lateral flow assay strips. *Sens Actuators B Chem.* 2018;270:72-79.
33 doi:10.1016/j.snb.2018.04.162
34
35
36 22. You M, Lin M, Gong Y, et al. Household Fluorescent Lateral Flow Strip Platform for Sensitive
37 and Quantitative Prognosis of Heart Failure Using Dual-Color Upconversion Nanoparticles.
38 *ACS Nano.* 2017;11(6):6261-6270. doi:10.1021/acsnano.7b02466
39
40
41 23. Zhang D, Huang L, Liu B, et al. Quantitative and ultrasensitive detection of multiplex cardiac
42 biomarkers in lateral flow assay with core-shell SERS nanotags. *Biosens Bioelectron.*
43 2018;106(January):204-211. doi:10.1016/j.bios.2018.01.062
44
45
46 24. Deng J, Yang M, Wu J, Zhang W, Jiang X. A Self-Contained Chemiluminescent Lateral Flow
47 Assay for Point-of-Care Testing. *Anal Chem.* 2018;90(15):9132-9137.
48 doi:10.1021/acs.analchem.8b01543
49
50
51 25. Fung KK, Chan CPY, Renneberg R. Development of enzyme-based bar code-style lateral-flow
52 assay for hydrogen peroxide determination. *Anal Chim Acta.* 2009;634(1):89-95.
53 doi:10.1016/j.aca.2008.11.064
54
55
56 26. Calabria D, Calabretta MM, Zangheri M, et al. Recent advancements in enzyme-based
57 lateral flow immunoassays. *Sensors.* 2021;21(10):1-19. doi:10.3390/s21103358
58
59
60

Analyst

ARTICLE

- 1
2
3
4
5 27. Sajid M, Kawde AN, Daud M. Designs, formats and applications of lateral flow assay: A
6 literature review. *Journal of Saudi Chemical Society*. 2015;19(6):689-705.
7 doi:10.1016/j.jscs.2014.09.001
8
- 9 28. Koczula KM, Gallotta A. Lateral flow assays. *Essays Biochem*. 2016;60(1):111-120.
10 doi:10.1042/EBC20150012
11
- 12 29. Chen A, Yang S. Replacing antibodies with aptamers in lateral flow immunoassay. *Biosens*
13 *Bioelectron*. 2015;71:230-242. doi:10.1016/j.bios.2015.04.041
14
- 15 30. Dalirirad S, Steckl AJ. Aptamer-based lateral flow assay for point of care cortisol detection in
16 sweat. *Sens Actuators B Chem*. 2019;283(August 2018):79-86.
17 doi:10.1016/j.snb.2018.11.161
18
- 19 31. Jauset-Rubio M, El-Shahawi MS, Bashammakh AS, Alyoubi AO, O'Sullivan CK. Advances in
20 aptamers-based lateral flow assays. *TrAC - Trends in Analytical Chemistry*. 2017;97:385-398.
21 doi:10.1016/j.trac.2017.10.010
22
- 23 32. Valdivia A, Torres I, Huntley D, et al. Qualitative assessment of SARS-CoV-2-specific antibody
24 avidity by lateral flow immunochromatographic IgG/IgM antibody assay. *J Med Virol*.
25 2021;93(2):1141-1144. doi:10.1002/jmv.26344
26
- 27 33. Tu D, Holderby A, Coté GL. Aptamer-based surface-enhanced resonance Raman scattering
28 assay on a paper fluidic platform for detection of cardiac troponin I. *J Biomed Opt*.
29 2020;25(9):097001-1-14. doi:10.1117/12.2544558
30
- 31 34. Kong D, Liu L, Song S, Zheng Q, Wu X, Kuang H. Rapid detection of tenuazonic acid in cereal
32 and fruit juice using a lateral-flow immunochromatographic assay strip. *Food Agric*
33 *Immunol*. 2017;28(6):1293-1303. doi:10.1080/09540105.2017.1337085
34
- 35 35. Lee LG, Nordman ES, Johnson MD, Oldham MF. A low-cost, high-performance system for
36 fluorescence lateral flow assays. *Biosensors (Basel)*. 2013;3(4):360-373.
37 doi:10.3390/bios3040360
38
- 39 36. Choi S, Hwang J, Lee S, Lim DW, Joo H, Choo J. Quantitative analysis of thyroid-stimulating
40 hormone (TSH) using SERS-based lateral flow immunoassay. *Sens Actuators B Chem*.
41 2017;240:358-364. doi:10.1016/j.snb.2016.08.178
42
- 43 37. Pan R, Jiang Y, Sun L, et al. Gold nanoparticle-based enhanced lateral flow immunoassay for
44 detection of *Cronobacter sakazakii* in powdered infant formula. *J Dairy Sci*.
45 2018;101(5):3835-3843. doi:10.3168/jds.2017-14265
46
- 47 38. Mahmoudi T, Shirdel B, Mansoori B, Baradaran B. Dual sensitivity enhancement in gold
48 nanoparticle-based lateral flow immunoassay for visual detection of carcinoembryonic
49 antigen. *Analytical Science Advances*. 2020;(March):1-12. doi:10.1002/ansa.202000023
50
51
52
53
54
55
56
57
58
59
60

- 1
2
3
4
5 39. Liu J, Hu X, Cao F, Zhang Y, Lu J, Zeng L. A lateral flow strip based on gold nanoparticles to
6 detect 6-monoacetylmorphine in oral fluid. *R Soc Open Sci.* 2018;5(6).
7 doi:10.1098/rsos.180288
8
- 9 40. Panraksa Y, Apilux A, Jampasa S, et al. A facile one-step gold nanoparticles enhancement
10 based on sequential patterned lateral flow immunoassay device for C-reactive protein
11 detection. *Sens Actuators B Chem.* 2020;(August):129241. doi:10.1016/j.snb.2020.129241
12
13
- 14 41. Ikeda K, Sakamoto Y, Kawasaki Y, et al. Determination of glycated albumin by enzyme-linked
15 boronate immunoassay (ELBIA). *Clin Chem.* 1998;44(2):256-263.
16
- 17 42. Testa R, Guerra E, Rita A, Gaetano N di, Santini G. Analytical Performances of an Enzymatic
18 Assay for the Measurement of Glycated Albumin. *Journal of Applied Laboratory Medicine.*
19 2016;01(02):162-171. doi:10.1373/jalm.2016.020446
20
21
- 22 43. Ko E, Tran VK, Geng Y, et al. Determination of glycated albumin using boronic acid-derived
23 agarose beads on paper-based devices. *Biomicrofluidics.* 2018;12(1):1-8.
24 doi:10.1063/1.5021395
25
- 26 44. Inoue Y, Inoue M, Saito M, Yoshikawa H, Tamiya E. Sensitive Detection of Glycated Albumin
27 in Human Serum Albumin Using Electrochemiluminescence. *Anal Chem.* 2017;89(11):5909-
28 5915. doi:10.1021/acs.analchem.7b00280
29
30
- 31 45. Bohli N, Meilhac O, Rondeau P, Gueffrache S, Mora L, Abdelghani A. A facile route to
32 glycated albumin detection. *Talanta.* 2018;184(November 2017):507-512.
33 doi:10.1016/j.talanta.2018.03.027
34
35
- 36 46. Ki H, Oh J, Han GR, Kim MG. Glycation ratio determination through simultaneous detection
37 of human serum albumin and glycated albumin on an advanced lateral flow immunoassay
38 sensor. *Lab Chip.* 2020;20(4):844-851. doi:10.1039/c9lc00967a
39
40
- 41 47. Ki H, Jang H, Oh J, et al. Simultaneous Detection of Serum Glucose and Glycated Albumin on
42 a Paper-Based Sensor for Acute Hyperglycemia and Diabetes Mellitus. *Anal Chem.* Published
43 online 2020:0-4. doi:10.1021/acs.analchem.0c02940
44
45
- 46 48. Apiwat C, Luksirikul P, Kankla P, et al. Graphene based aptasensor for glycated albumin in
47 diabetes mellitus diagnosis and monitoring. *Biosens Bioelectron.* 2016;82:140-145.
48 doi:10.1016/j.bios.2016.04.015
49
- 50 49. Gosh S, Datta D, Cheema M, Dutta M, Stroschio M. Aptasensor based optical detection of
51 glycated albumin for diabetes mellitus diagnosis. *Nanotechnology.* 2017;28:435505-435516.
52
53
- 54 50. Kouzuma T, Usami T, Yamakoshi M, Takahashi M, Imamura S. An enzymatic method for the
55 measurement of glycated albumin in biological samples. *Clinica Chimica Acta.* 2002;324(1-
56 2):61-71. doi:10.1016/S0009-8981(02)00207-3
57
58
59
60

Analyst

ARTICLE

- 1
2
3
4
5 51. Mudanyali O, Dimitrov S, Sikora U, Padmanabhan S, Navruz I, Ozcan A. Integrated rapid-
6 diagnostic-test reader platform on a cellphone. *Lab Chip*. 2012;12(15):2678-2686.
7 doi:10.1039/c2lc40235a
8
- 9 52. Joung HA, Ballard ZS, Wu J, et al. Point-of-Care Serodiagnostic Test for Early-Stage Lyme
10 Disease Using a Multiplexed Paper-Based Immunoassay and Machine Learning. *ACS Nano*.
11 2020;14(1):229-240. doi:10.1021/acsnano.9b08151
12
13
- 14 53. Land KJ, Boeras DI, Chen XS, Ramsay AR, Peeling RW. REASSURED diagnostics to inform
15 disease control strategies, strengthen health systems and improve patient outcomes. *Nat*
16 *Microbiol*. 2019;4(1):46-54. doi:10.1038/s41564-018-0295-3
17
18
- 19 54. Bastús NG, Comenge J, Puntès V. Kinetically controlled seeded growth synthesis of citrate-
20 stabilized gold nanoparticles of up to 200 nm: Size focusing versus ostwald ripening.
21 *Langmuir*. 2011;27(17):11098-11105. doi:10.1021/la201938u
22
23
- 24 55. Belsare S, Coté G. Development of paper-based colorimetric assays for monitoring
25 gestational diabetes at the point-of-care. *Proceedings of SPIE*. 2021;11651(March):21.
26 doi:10.1117/12.2585542
27
- 28 56. Liu B, Liu J. Methods for preparing DNA-functionalized gold nanoparticles, a key reagent of
29 bioanalytical chemistry. *Analytical Methods*. 2017;9(18):2633-2643.
30 doi:10.1039/c7ay00368d
31
- 32 57. Bahadır EB, Sezgintürk MK. Lateral flow assays: Principles, designs and labels. *TrAC - Trends*
33 *in Analytical Chemistry*. 2016;82:286-306. doi:10.1016/j.trac.2016.06.006
34
35
- 36 58. López-Marzo AM, Pons J, Blake DA, Merkoçi A. High sensitive gold-nanoparticle based
37 lateral flow Immunodevice for Cd²⁺-detection in drinking waters. *Biosens Bioelectron*.
38 2013;47:190-198. doi:10.1016/j.bios.2013.02.031
39
40
41
42
43
44
45
46
47
48
49
50
51
52
53
54
55
56
57
58
59
60